Dynamically Amplified Dual-mass Gyroscopes with In-situ Shock Survival Mechanism

Danmeng Wang, Radwan M. Noor, and Andrei M. Shkel
MicroSystems Laboratory, Department of Mechanical and Aerospace Engineering
University of California, Irvine, CA 92697, USA
Email: {*danmenw, rmmohamm, ashkel*}@uci.edu

***Abstract*—This paper reports on development of Dynamically Amplified dual-mass Gyroscope (DAG) and introduces, for the first time, a Trap-and-Hold (TAH) concept intended to increase survivability of gyroscopes to mechanical shocks and vibrations. The TAH concept utilizes out-of-plane electrodes to electrostatically excite the gyroscope's proof-mass at resonance in the direction perpendicular to the substrate, trap the proof-mass electrostatically, and then keep the sensor structure locked to the substrate during the events of shock. We discuss our fabrication process to realize the TAH mechanism and present initial experimental results. In our demonstration, the operational device measuring rotation was instantaneously immobilized by TAH before the event of shock, and was subsequently released to its normal operation after the event of shock. The device preserved its functionality and fundamental characteristics, Angle Random Walk (ARW) and in-run bias instability (IrBS), before (ARW: 0.048 deg/rt-hr, IrBS: 0.6 deg/hr) and after the experiment (ARW: 0.0483 deg/rt-hr, IrBS: 0.69 deg/hr).**

Keywords: MEMS gyroscopes, dynamic amplification, dual-mass gyroscope, shock survivability, through-glass-via

I. Introduction

MEMS inertial sensors are good candidates for operation in extreme environments due to their relatively small size and mass. However, it is a challenge for high performance gyroscope devices to be immune to shocks while preserving sensitivity. In this paper, we propose a shock survivability strategy intended for Dynamically Amplified dual-mass Gyroscopes (DAG), a specific class of high performance gyroscopes reported in [1]. DAGs, similar to any other gyroscopes designed for high performance, operate at a relatively low operational frequency, on the level of 5 kHz, for effective electrostatic tunability and high signal-to-noise ratio. The devices are therefore susceptible to mechanical shock due to their increased proof-mass and weak suspension. For shock survivability, gyroscope structures need to be stiffened. Devices having high operational frequencies (>200 kHz) may capable of withstanding large magnitude shocks without any protection, [2]. An increase in stiffness limits gyroscope's amplitude of response, thus affecting sensitivity and tunability. The increased stiffness is also a hindrance to implement the dynamic amplification concept [3].

The reported Trap-and-Hold (TAH) architecture is an add-on mechanism to DAG architecture to improve shock resistance of the device. It utilizes out-of-plane electrodes along the non-operational mode to selectively trap the proof-mass before the events of shock, effectively immobilizing the device in preparation for shocks. The proposed implementation is similar to the dynamic switching idea used in bistable mechanisms, [4], where the two stable modes of a device are: a high sensitivity operational mode and a Shock-Lock mode for shock survival. It should be noted, the shock survival approach presented in this paper is intended for switching to the Shock-Lock mode before the events of shock and is not intended for operation-through-shock. A high performance DAG design with parameters documented in [1] was chosen for the proof of concept. A prototype of TAH integrated with a DAG is shown in Fig. 1(a).

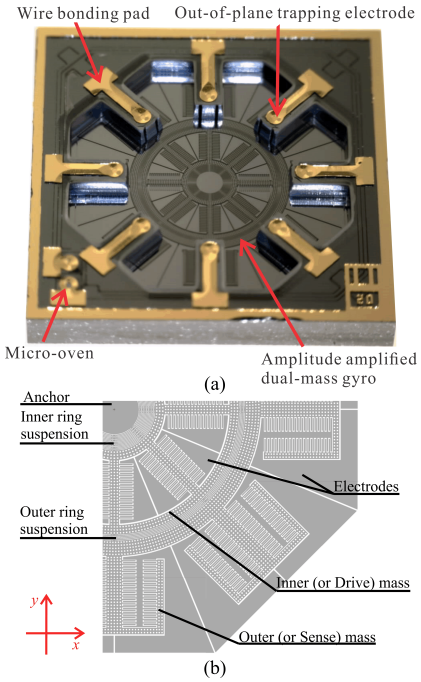

Fig. 1. (a) A prototype of the dual-mass gyroscope bonded to the cap stage with thru-wafer interconnects serving as in-situ shock survival mechanism. (b) Close-up of a quarter of the amplitude amplified dual-mass device.

II. Dynamically Amplified Gyroscope

The dynamic amplification concept promises a higher sensitivity by utilizing an increased number of degrees of freedom (DOF) to achieve the amplitude amplification, [5], Fig.

This material is based on work supported by the Defense Advanced Research Projects Agency and U.S. Navy under contract No. N66001-16-1-4021.

978-1-7281-2983-9/20/$31.00 ©2020 IEEE

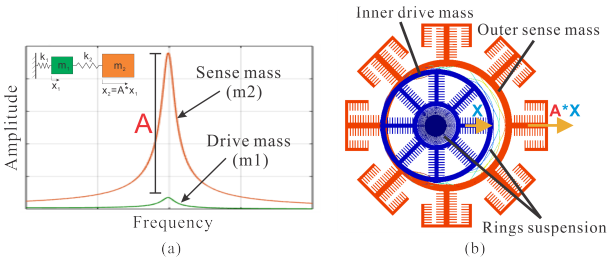

Fig. 2. (a) Frequency response of a dual mass-spring structure with dynamic amplification. By actuating the drive mass, m_1, a A time larger amplitude of the sense mass, m_2, is achieved. (b) FEA model of the dynamically amplified dual-mass structure, showing operational modes along the drive-mode direction (x-axis).

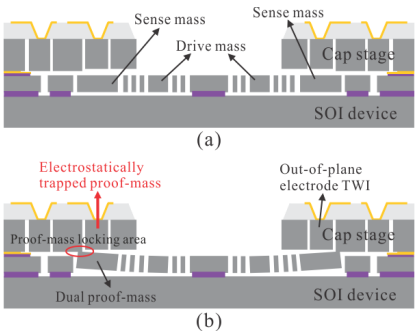

Fig. 3. Schematic diagram of TAH concept. (a) Normal position of the dual-mass gyroscope before and after TAH (Normal Operation). (b) TAH engaged, immobilizing the sensor throughout the duration of shock (Shock-Lock).

2(a). We adopted the concentric ring suspension dual-mass design in our DAG, which comprises an inner drive-mass (m_1) attached to a central anchor and connected to an outer sense-mass (m_2) by concentric ring suspensions (k_1 and k_2), Fig. 1(b), [6]. Through carefully picking the stiffness-to-mass ratio, a dynamically amplified amplitude factor of A can be achieved, shown in Eq. (1). The operational modes of DAG are schematically illustrated in Fig. 2(b), showing A times amplitude amplification of the sense mass along the x-axis:

$$A = \frac{x_2}{x_1} = \frac{\omega_2^2}{\omega_2^2 - \omega^2 + j\omega\frac{c_2}{m_2}} \quad (1)$$

In Eq. (1), x_1 is a displacement of the drive mass and x_2 is a displacement of the sense mass, both along the x-axis. c_2 is the damping coefficient associated with the sense mass and ω is the applied frequency of excitation. The frequency ω_2 is equal to $\sqrt{k_2/m_2}$. The dual-mass architecture is able to possess a larger amplitude of response, allowing actuation with smaller (more linear) amplitude and achieving an increased sensitivity.

III. Design and Fabrication

A. Trap-and-Hold concept

Trap-and-Hold (TAH) is a proposed add-on feature to enhance shock survivability of gyroscopes while preserving their high sensitivity. The concept utilizes a second stable mode, Shock-Lock mode, Fig. 3(b), in addition to the usual gyroscope's operational mode, Fig. 3(a).

A typical TAH-engaged operation is demonstrated in Fig. 3. At the beginning, the device is in its neutral position or in the Normal Operation mode, Fig. 3(a). Right before the event of shock, the device is transitioned from the Normal Operation mode to the Shock-Lock mode. A DC voltage is applied to the out-of-plane electrodes to actuate the proof-mass perpendicular to the substrate at the out-of-plane resonance frequency, driving the edge of the proof-mass to make a contact and temporary immobilizing the structure. The device remains at its Shock-Lock mode throughout the event of shock, Fig. 3(b). After the shock, the electrostatic DC voltage is removed to allow a transition of the proof-mass from the Shock-Lock mode back to the Normal Operation mode. As the proof-mass is released to return to its neutral position, the device restores its normal operation of the angular rate sensing.

B. Fabrication Process

The fabrication process for the cap wafer, shown in Fig. 4, includes the following steps: Step (1): anodic bonding of an 100 μm thick Pyrex wafer to a 500 μm Si wafer; Step (2): 10% HF wet etching for thru-wafer interconnects (TWI) with 200 nm Au layer as a hard mask; Step (3): E-beam metalization and patterning of Cr/Au on both sides of the cap wafer, which serves as top wire-bonding paths and bottom bonding pads; Step (4) and Step (5): Deep Reactive Ion Etching (DRIE) of Si on the cap wafer to create out-of-plane gaps (3 μm) and to insulate electrodes. The resulting TWI cap wafer contains the out-of-plane electrodes to trap and hold the device's proof-mass against shocks and at the same time to provide the electrically insulated locking area.

An additional step in the fabrication process of the sensor is required for bonding of the cap stage to the device. Our standard in-house SOI fabrication process was used to process the SOI device wafer, Step (II-IV) in Fig. 4, with an addition of Step (I): deposition of a Cr/Au layer as bonding pads. The SOI wafer, which was used for fabrication of devices, consisted of a 50 μm thick Si device layer, a 500 μm thick handle wafer, and a 5 μm thick buried oxide layer between them.

The cap wafer was bonded to the SOI wafer using Au-to-Au thermo-compression bonding process in AML-AWB 4" wafer bonder allowing less than 20 μm between-wafer misalignment in the horizontal direction, Fig. 3(a). The device contains a total of 8 out-of-plane electrodes for TAH and a central opening to access in-plane electrodes on the device layer, necessary for the gyroscope operation, Fig. 1(a).

In this paper, we also demonstrated an improved fabrication process, illustrated in Fig. 5. The process forms a cap wafer defining Through-Glass-Vias (TGVs) intended for both in- and out-of-plane electrodes and vacuum packaging of the device wafer on the wafer-level. Step (a): DRIE Si etching of 500 μm thick silicon wafer to a depth of 250 μm, which is a 100 mm in diameter, <1-0-0> orientation, and 1-5 Ohm-cm resistivity; Step (b): anodic bonding of the etched Si wafer to a 250 μm thick Borofloat® 33 glass wafer with AML-AWB 4" wafer bonder under pressure <1 mTorr to create vacuum in the encapsulated cavities; Step (c): 4 hours long glass reflow

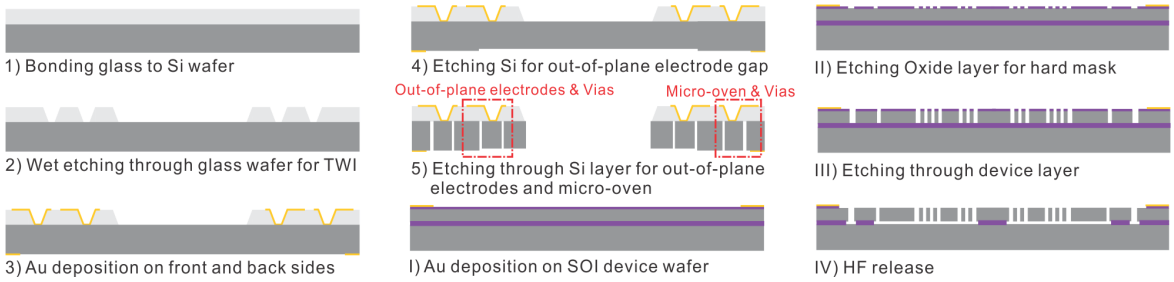

Fig. 4. The reported fabrication process for implementation of a gyroscope with out-of-plane TAH electrodes.

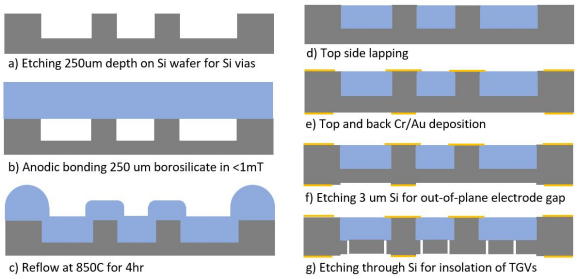

Fig. 5. The improved fabrication process for dust-free cap wafer with integrated in- and out-of-plane Through-Glass-Via electrodes.

in a 850 °C annealing furnace; Step (d): lapping of the bonded wafer from the glass side until Si surface is exposed; Step (e): top and bottom metallization and patterning (500 nm Au with 50 nm Cr) for wire bonding pads (top) and Au-to-Au bonding pads for thermal compression bonding (bottom); Step (f): DRIE of backside Si to create out-of-plane gap of 3 μm; Step (g): etch through the remaining 250 μm Si to insulate TGVs. The process was successfully implemented for forming the cap wafer, shown in Fig. 6(a) and (b), allowing for a dust-free and ultimately for an in-vacuum operating condition, in addition to providing electrical interconnects. Fig. 6(c) illustrates the assembly of the cap stage to a metallized DAG, Fig. 6(a) bottom, using Au-to-Au thermal compression bonding. Initial characterization of the cap stage with a DAG was performed on a probe station under atmospheric pressure. Frequency sweeps of inner and outer masses were characterized using a Zurich lock-in amplifier, Fig. 7. The experimental test verified an operation of the 4 DOFs structure with 16 functional in-plane TGV electrodes.

IV. TAH Evaluation

A. Experimental Setup

A prototype with bonded DAG to the cap stage, Fig. 1(a), was attached to a LCC package and mounted on a front-end circuit board. An accelerometer, ADXL356, was affixed on the backside of the front-end circuit to measure the shock applied to the board, and thus the tested gyroscope. The configuration was tested in a vacuum chamber assembled on a rate table, which was harmonically driven at an amplitude of 3.75 deg/s. The gyroscope was operated in an open-loop rate mode along the sense axis with Phase-Locked Loop and Amplitude Gain Control Loop stabilization along the drive axis. The device was

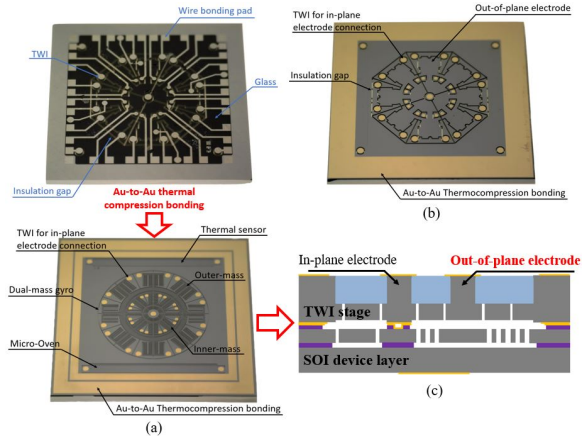

Fig. 6. (a) Thermal compression bonding of the cap stage (top) to a metallized DAG (bottom). (b) The back side of the cap stage. Glass on the front side, (a) top, provides mechanical integrity to the structure and the 500 nm Au layer on the back side defines as the bonding pads. (c) Schematic diagram of the packaging process for device encapsulation.

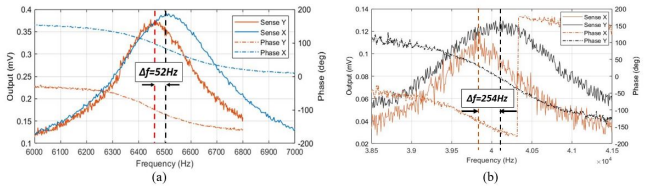

Fig. 7. Frequency sweeps of (a) outer sense mass and (b) inner drive mass of the DAG prototype in X and Y directions, tested under atmospheric pressure. The device was encapsulated using the process described in Fig. 5

excited at its 3.6 kHz in-plane operational frequency, defined as the gyroscope's Normal Operation mode. The gyroscope had an as-fabricated frequency split of 14 Hz, which was tuned down to 1 Hz using the electrostatic compensation method described in [7]. The quality factor of the device was 110k with 11x amplitude amplification.

As a preliminary demonstration of the concept, shocks were applied from outside of the vacuum chamber by a lightweight shock inducing hammer. The shock was transferred from outside to inside of the chamber reaching the front-end circuit with some energy loss, and the transferred shock was measured by the accelerometer attached to the circuit board. Due to safety concerns and for protection of the experimental equipment, the maximum within-chamber shock was limited to about 5g. Nonetheless, 5g shock was sufficient to induce

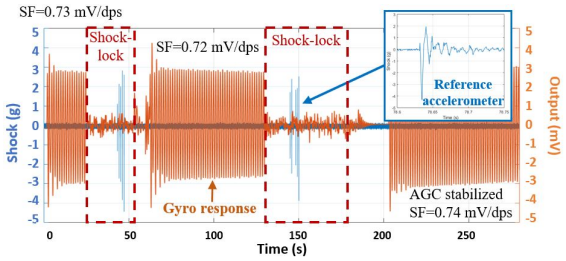

Fig. 8. Initial demonstration of the TAH strategy on a DAG prototype. Orange line is the measured response from the gyroscope; blue line represents readouts from the reference accelerometer monitoring the events of shock.

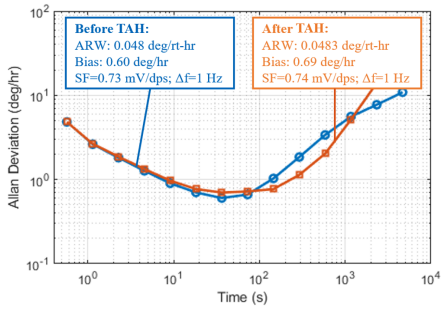

Fig. 9. The Allan Deviation of the DAG prototype (tested in a vacuum chamber) in the open-loop operational mode before and after TAH.

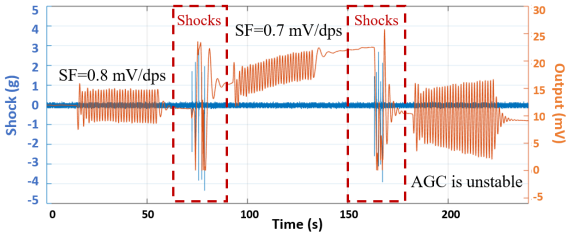

Fig. 10. The experimental illustration of the gyroscope response to a harmonic excitation amplitude of 3.75 deg/s before and after in-plane shocks. Orange line is the measurement of gyroscope's response; blue line is the output of the reference accelerometer.

sensor drifts and alter the fundamental characteristics to the degree where re-calibration of the sensor would be required. Notably, during our experiments, detrimental collisions of electrode structures occurred due to shocks as low as 3g, since the design utilized a larger proof-mass and low operational frequency to achieve a high sensitivity of operation.

B. Experimental Results

The prototype was in the Normal Operation mode with an initial measured sensitivity to rotation of 0.73 mV/dps (Fig. 8, from 0 to 25 sec). At 25 sec, an out-of-plane electrostatic trapping force was applied, driving the proof mass at its out-of-plane resonance of 1.91 kHz to lock and immobilize the structure, activating the Shock-Lock mode. Then, the rotation stimulus was removed (Fig. 8, from 30 to 50 sec), followed by few in-plane shocks up to 4.5g with 8 msec half-sine duration (Fig. 8, from 40 to 45 sec). After releasing the proof-mass (Fig. 8, from 53 to 60 sec), the device returned gradually to its neutral position and continued its normal operation with the sensitivity of 0.72 mV/dps, until the end of the duration of 130 sec. The process was repeated multiple times. The Angle Random Walk (ARW) and in-run bias instability (IrBS) characteristics, before TAH and after repeated TAH operations, are shown in Fig. 9. The measured ARW before the shock was 0.048 deg/rt-hr and IrBS was 0.6 deg/hr. The after-shock measured ARW was 0.0483 deg/rt-hr and the measured IrBS was 0.69 deg/hr. A slight deviation in bias instability is explained by uncompensated variations in temperature during experiments.

For comparison, the same characterization procedures were repeated on the same gyroscope without switching to Shock-Lock mode before the events of shock, Fig. 10. Due to the low operational frequency, the output signal convulsed for the duration of excitation (Fig. 10, from 70 to 85 and from 150 to 170 sec), and the sensor was not able to recover its performance after the events of shock (Fig. 10, from 85 to 130 and from 180 to 240 sec), emphasizing the relevance of the TAH concept for augmenting shock performance of gyroscopes.

V. Conclusion

The TAH strategy was demonstrated to improve the gyroscope's shock survivability while preserving its noise characteristics. Additionally, we described a process for dust-proof cap stage with experimentally demonstrated electrical interconnects with both in- and out-of-plane TGVs using an in-house glass reflow process.

Acknowledgment

This material is based on work supported by the Defense Advanced Research Projects Agency and U.S. Navy under contract No. N66001-16-1-4021. Devices were designed and characterized at UCI Microsystems Laboratory and fabricated at UCI INRF cleanroom facility. The work of R. M. Noor was supported by King AbdulAziz City for Science and Technology (KACST).

References

[1] D. Wang, A. Efimovskaya, and A. M. Shkel, "Amplitude Amplified Dual-Mass Gyroscope: Design Architecture and Noise Mitigation Strategies," in *IEEE International Symposium on Inertial Sensors and Systems (INERTIAL)*, Naples. FL, USA, April 1-5 2019.

[2] S. W. Yoon, "Vibration isolation and shock protection for MEMS." Ph.D. dissertation, University of Michigan, 2009.

[3] C. W. Dyck, J. J. Allen, and R. J. Huber, "Microelectromechanical dual-mass resonator structure," May 28 2002, US Patent 6,393,913.

[4] J. Casals-Terre and A. Shkel, "Dynamic analysis of a snap-action micromechanism," in *IEEE Sensors Conference*, Vienna, Austria, Oct 24-27 2004.

[5] C. C. Painter and A. M. Shkel, "Dynamically amplified rate integrating gyroscope," Aug. 16 2005, US Patent 6,928,874.

[6] D. Wang, M. H. Asadian, A. Efimovskaya, and A. M. Shkel, "A comparative study of conventional single-mass and amplitude amplified dual-mass MEMS Vibratory Gyroscopes," in *IEEE International Symposium on Inertial Sensors and Systems (INERTIAL)*, Kauai. HI, USA, March 27-30 2017.

[7] A. Efimovskaya, D. Wang, Y.-W. Lin, and A. M. Shkel, "Electrostatic compensation of structural imperfections in dynamically amplified dual-mass gyroscope," *Sensors and Actuators A: Physical*, vol. 275, pp. 99–108, 2018.